Density excitations of a harmonically trapped ideal gas

JAI CAROL CRUZ[1,†], C N KUMAR[1], K N PATHAK[1,*] and J BOSSE[2]

[1]Department of Physics, Panjab University, Chandigarh 160 014, India
[2]Institute of Theoretical Physics, Freie Universität Berlin, Berlin, Germany
*Corresponding author. E-mail: pathak@pu.ac.in

Abstract. The dynamic structure factor $S(\mathbf{q}, \omega)$ of a harmonically trapped Bose gas has been calculated well above the Bose–Einstein condensation temperature by treating the gas cloud as a canonical ensemble of non-interacting classical particles. The static structure factor is found to vanish $\propto q^2$ in the long-wavelength limit. We also incorporate a relaxation mechanism phenomenologically by including a stochastic friction force to study $S(\mathbf{q}, \omega)$. A significant temperature dependence of the density fluctuation spectra is found. The Debye–Waller factor has been calculated for the trapped thermal cloud as a function of q and the number $\mathcal{N}$ of atoms. A substantial difference is found for small- and large-$\mathcal{N}$ clouds.

1. Introduction

For more than a decade, there has been much interest in the study of trapped atomic gases [1,2]. Experimentalists have observed not only density profiles of these systems but also successfully detected particle-number and particle-density fluctuations in ultracold atomic gases [3]. Progress has been made in understanding spatial and temporal correlations of density fluctuations in a variety of inhomogeneous cold-atom systems [4–7] for $T = 0$ as well as below the Bose–Einstein condensation (BEC) temperature T_c. In addition there have been extensive studies of dynamical density fluctuations for homogeneous systems [8,9].

The purpose of this work is to calculate the diagonal elements of the matrix of time-dependent correlation functions of density fluctuations for a harmonically

---

†Worked as a summer student fellow of the Indian Academy of Sciences for six weeks.

trapped classical ideal gas, which determine the coherent scattering properties of the system. Motivation for calculating the dynamical structure factor is its expected strong temperature dependence which could be useful to estimate the cloud temperature experimentally. Moreover, the exactly solvable model not only provides the limiting case of a system in the absence of interactions but also furnishes a useful result for trapped dilute gases well above the BEC temperature. Justification for a classical treatment is based on the fact that for an atom trap of typical trap frequency $\Omega = 120 \times 2\pi \, \text{s}^{-1}$ containing $\mathcal{N} = 2 \times 10^4$ rubidium atoms which implies the critical temperature $T_c = \hbar\Omega\mathcal{N}^{1/3}/[\zeta(3)^{1/3}k_B] \approx 147 \, \text{nK}$ of Bose–Einstein condensation ([1], Chap. 2.2), the ratio $\hbar\Omega$ over $k_B T$ is very small in the temperature range well above T_c, where many experiments are performed, because $\hbar\Omega/(k_B T_c) \approx 0.04$. Moreover, at these temperatures the reduced density $\rho = n\lambda^3 \approx 0.01$ is small implying $\lambda \approx 0.008L$, i.e. the de Broglie wavelength λ is still very small compared to the linear extension L of the atom cloud.

In addition to the restoring force acting on each particle due to the trap potential, we allow for a frictional force when studying the dynamical behaviour of the trapped gas. Simultaneously, a time-dependent random force is assumed to act on each oscillator. This stochastic force will keep particles moving, thus preventing them from being slowed down by friction and coming to a rest in the trap-potential minimum. Thermal averages are therefore understood to include additional averaging over stochastic variables. In this way, the assumption of time-translational invariance will remain justified throughout in spite of frictional forces.

In §2, we present the basic definitions and the correlation functions to be studied. In §3, the one- and two-particle densities and the static structure factor are obtained. In §4, the intermediate scattering function has been calculated in the presence of damping including a stochastic force with Gaussian noise. Resulting low-friction density-relaxation spectra are discussed as a function of temperature. In §5, density excitations for the limiting case of zero friction and the Debye–Waller factor (DWF) are discussed. Finally, concluding remarks are given in §6.

2. Theoretical considerations

In the description of dynamical properties of a many-particle system, the correlation function of density fluctuations $\delta N(\mathbf{r}, t)$,

$$F(\mathbf{r}, \mathbf{r}', t) = \frac{1}{\mathcal{N}} \langle \, \delta N(\mathbf{r}, t) \, \delta N(\mathbf{r}', 0) \, \rangle, \tag{1}$$

and its spatial Fourier transform

$$F_{\mathbf{q}\,\mathbf{q}'}(t) = \int \mathrm{d}^3 r \int \mathrm{d}^3 r' \; \mathrm{e}^{-i\mathbf{q}\cdot\mathbf{r}+i\mathbf{q}'\cdot\mathbf{r}'} F(\mathbf{r}, \mathbf{r}', t) = \frac{1}{\mathcal{N}} \langle \delta N_{\mathbf{q}}(t) \, \delta N_{\mathbf{q}'}(0)^* \rangle \tag{2}$$

play important roles. Here $\langle \cdots \rangle$ denotes a thermal equilibrium average, and the dynamical variable $N(\mathbf{r}, t) = \sum_{j=1}^{\mathcal{N}} \delta(\mathbf{r} - \mathbf{r}_j(t))$ describes the particle density at space point $\mathbf{r}$ and time t, which, when integrated over all space, sums up to the

total number of particles, $\mathcal{N} = \int \mathrm{d}^3 r\, N(\mathbf{r}, t)$. Correspondingly, the density variable in Fourier space is given by

$$N_{\mathbf{q}}(t) = \int \mathrm{d}^3 r\, \mathrm{e}^{-\mathrm{i}\mathbf{q}\cdot\mathbf{r}}\, N(\mathbf{r}, t) = \sum_{j=1}^{\mathcal{N}} \mathrm{e}^{-\mathrm{i}\mathbf{q}\cdot\mathbf{r}_j(t)} \tag{3}$$

with fluctuation $\delta N_{\mathbf{q}}(t)$. The thermal fluctuation of a dynamical variable $A(t)$ is defined as $\delta A(t) \equiv A(t) - \langle A(t)\rangle = A(t) - \langle A\rangle$, where invariance of the thermal equilibrium state with respect to time translations renders $\langle A(t)\rangle$ independent of time t.

The diagonal elements $F(\mathbf{q}, t) = F_{\mathbf{q}\mathbf{q}}(t)$ are known as intermediate scattering functions, because they determine the double-differential coherent-scattering cross-section observed when neutrons or photons are scattered from the system. The cross-section is proportional to $\int_{-\infty}^{\infty} \mathrm{d}t\, \exp(\mathrm{i}t\omega) \langle N_{\mathbf{q}}(t) N_{\mathbf{q}}(0)^*\rangle$. It is conventionally written as [10]

$$\left(\frac{\mathrm{d}^2\sigma}{\mathrm{d}\omega\,\mathrm{d}\hat{\Omega}}\right)^{\mathrm{coh}} = \frac{p_f}{p_i}\, a^2 \left[\frac{|\langle N_{\mathbf{q}}\rangle|^2}{\mathcal{N}}\, \delta(\omega) + S(\mathbf{q}, \omega)\right] \tag{4}$$

by introducing the van Hove function

$$S(\mathbf{q}, \omega) = \frac{1}{2\pi} \int_{-\infty}^{\infty} \mathrm{d}t\, \mathrm{e}^{\mathrm{i}t\omega} F(\mathbf{q}, t). \tag{5}$$

In the coherent-scattering cross-section eq. (4), $\hbar\mathbf{q} = \mathbf{p}_i - \mathbf{p}_f$ and $\hbar\omega = E_i - E_f$ denote the momentum and the energy, respectively, which is transferred in a scattering process from the projectile (neutron, e.g.) to the target system (gas), and a denotes the coherent scattering length of the gas.

We note that the right-hand side of eq. (4) will represent a decomposition into elastic and inelastic scattering contributions if, and only if, $F(\mathbf{q}, \infty) = 0$ implying an ergodic many-particle system. For non-ergodic systems with $F(\mathbf{q}, \infty) > 0$, the van Hove function $S(\mathbf{q}, \omega)$ itself will have an elastic peak of strength $F(\mathbf{q}, \infty)$ in addition to inelastic $(\omega \neq 0)$ contributions. As will be shown below, the harmonically trapped ideal gas represents not only an inhomogeneous but also a non-ergodic many-particle system.

In general, the elastic coherent-scattering intensity is measured by the DWF defined as the ratio of elastic and total coherent-scattering intensity,

$$f(\mathbf{q}) = \lim_{t\to\infty} \frac{\langle N_{\mathbf{q}}(t) N_{\mathbf{q}}^*\rangle}{\rangle} \langle |N_{\mathbf{q}}|^2\rangle = \frac{|\langle N_{\mathbf{q}}\rangle|^2/\mathcal{N} + F(\mathbf{q}, \infty)}{|\langle N_{\mathbf{q}}\rangle|^2/\mathcal{N} + F(\mathbf{q}, 0)}\,. \tag{6}$$

Here

$$F(\mathbf{q}, 0) = \int_{-\infty}^{\infty} \mathrm{d}\omega\, S(\mathbf{q}, \omega) \equiv S(\mathbf{q}) = \frac{1}{\mathcal{N}} \langle |\delta N_{\mathbf{q}}|^2\rangle \tag{7}$$

is the well known static structure factor $S(\mathbf{q})$. We emphasize that no assumptions regarding translational invariance of the target system have been made in the above

equations. We note that in eq. (6) there are two contributions to the DWF, in general. It is worth recalling that for a crystalline solid the first contribution is non-zero, while the second, i.e. $F(\mathbf{q}, \infty)$, vanishes since the crystalline solid is an ergodic system. On the other hand, for a non-ergodic (structural) glass $F(\mathbf{q}, \infty) > 0$, and $\langle N_{\mathbf{q}} \rangle$ is zero for all $\mathbf{q} \neq 0$ in the homogeneous system. In a homogeneous fluid, both contributions are zero resulting in a vanishing DWF. However, in the inhomogeneous trapped gas studied here, there will be a finite DWF as shown in §5.

Although $F_{\mathbf{qq'}}(t)$ for an inhomogeneous system will generally be non-zero if $\mathbf{q} \neq \mathbf{q'}$, only the diagonal elements are required for calculating the coherent double-differential scattering cross-section. That is, the intermediate scattering function $F(\mathbf{q}, t) = F_{\mathbf{qq}}(t)$ will determine the coherent-scattering cross-section (aside from the average density, which is responsible for the elastic 'Bragg-scattering' contribution of strength $|\langle N_{\mathbf{q}} \rangle|^2 / \mathcal{N}$).

We now consider a system of $\mathcal{N}$ non-interacting particles of mass m moving in three-dimensional space under the influence of an isotropic harmonic external potential. This collection of oscillators is described by the Hamiltonian

$$H = \sum_{j=1}^{\mathcal{N}} \left[\frac{\mathbf{p}_j^2}{2m} + V(\mathbf{r}_j) \right], \tag{8}$$

where $V(\mathbf{r}) = \frac{1}{2} m \Omega^2 \mathbf{r}^2$ with oscillator frequency Ω, and $\mathbf{p}_j$ and $\mathbf{r}_j$ denote momentum and position variables of the jth particle, respectively. For the trapped ideal gas described by eq. (8), thermal averages of additive single-particle variables of the general form $A(t) := \sum_{j=1}^{\mathcal{N}} A(\mathbf{p}_j(t), \mathbf{r}_j(t))$ reduces to the simple expression

$$\langle A(t) \rangle = \mathcal{N} \int \mathrm{d}^3 \hat{p} \, \frac{\exp\left(-\hat{\mathbf{p}}^2 / 2 p_{\mathrm{T}}^2\right)}{\left(p_{\mathrm{T}} \sqrt{2\pi}\right)^3} \int \mathrm{d}^3 \hat{r} \, \frac{\exp\left(-\hat{\mathbf{r}}^2 / 2 u^2\right)}{\left(u \sqrt{2\pi}\right)^3} \, A(\hat{\mathbf{p}}(t), \hat{\mathbf{r}}(t)), \tag{9}$$

where $p_{\mathrm{T}} = m v_{\mathrm{T}}$, $v_{\mathrm{T}} = \sqrt{k_{\mathrm{B}} T / m}$ and $u = v_{\mathrm{T}} / \Omega$ denote, respectively, the particle's thermal momentum, thermal speed and distance travelled within time Ω^{-1}. In general, $\hat{\mathbf{r}}(t) = \mathbf{R}(\hat{\mathbf{p}}, \hat{\mathbf{r}}; t)$ and $\hat{\mathbf{p}}(t) = \mathbf{P}(\hat{\mathbf{p}}, \hat{\mathbf{r}}; t)$ will depend on initial momentum $\hat{\mathbf{p}}$, initial position $\hat{\mathbf{r}}$ and time t. The vector-valued functions $\mathbf{R}$ and $\mathbf{P}$ will be determined from Hamilton's equations of motion in §4 below. For $t = 0$, however, $\hat{\mathbf{r}}(0) = \hat{\mathbf{r}}$ and $\hat{\mathbf{p}}(0) = \hat{\mathbf{p}}$. The evaluation of the six-fold integral on the right-hand side of eq. (9) is straightforward then. The static averages entering eqs (4), (6) and (7) are discussed in §3.

3. Static correlations

Using eq. (9), one obtains for the average particle-number density,

$$\langle N(\mathbf{r}) \rangle = \frac{\mathcal{N} \exp\left(-\mathbf{r}^2 / 2 u^2\right)}{\left(u \sqrt{2\pi}\right)^3} \quad \longleftrightarrow \quad \langle N_{\mathbf{q}} \rangle = \mathcal{N} \mathrm{e}^{-(1/2) q^2 u^2}. \tag{10}$$

We also note that the mean-square displacement of a particle from the centre of the trap is

$$\langle \mathbf{r}_0^2 \rangle = \left\langle \frac{1}{\mathcal{N}} \sum_{j=1}^{\mathcal{N}} \mathbf{r}_j^2 \right\rangle = 3u^2, \tag{11}$$

rendering an additional physical interpretation of the length u. According to eqs (10) and (11), in thermal equilibrium the trapped gas will form a spherically symmetric cloud in which $90.0(99.0; 99.9)\%$ of the gas particles are contained in a sphere of radius $a \approx 2.5(3.4; 4.0)u$ around the centre of force.

For the initial value $F_{\mathbf{qq'}}(0)$ describing the static correlations of density fluctuations, one finds (see also eqs (16) and (17) below):

$$F_{\mathbf{qq'}}(0) = \frac{1}{\mathcal{N}} \langle \delta N_{\mathbf{q}} \, \delta N_{\mathbf{q'}}^* \rangle = \mathrm{e}^{-(1/2)(q^2 + q'^2)u^2}(\mathrm{e}^{\mathbf{q} \cdot \mathbf{q'} \, u^2} - 1). \tag{12}$$

The corresponding result in $\mathbf{r}$-space is given in Appendix B. Note the symmetry relation, $F_{\mathbf{qq'}}(0) = F_{\mathbf{q'q}}(0)$, and the vanishing small-q limit, $\lim_{q \to 0} F_{\mathbf{qq'}}(0) = 0$.

At this stage, let us point out an interesting fact regarding the static structure factor defined in eq. (7) which, for the trapped ideal gas, can be read from the diagonal elements of eq. (12):

$$S(\mathbf{q}) = 1 - \mathrm{e}^{-q^2 u^2}. \tag{13}$$

As displayed in figure 1a, $S(q) \to q^2 u^2 + \mathcal{O}(q^4)$ for long wavelengths. Lacking a well-defined volume occupied by $\mathcal{N}$ particles, an overall particle-number density n cannot rigorously be defined in the inhomogeneous gas. However, the 'peak density'

$$n_0 := \langle N(\mathbf{r}{=}0) \rangle = \frac{\mathcal{N}}{L^3}, \quad L := u\sqrt{2\pi} \tag{14}$$
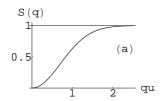
presents a reasonable measure of the overall density. Due to the rapidly decreasing average density $\langle N(\mathbf{r}) \rangle$ for $|\mathbf{r}| > u$ (see eq. (10)), $V = L^3$ will be considered to represent the gas volume. It corresponds to a sphere of radius $a = 3^{1/3}(\pi/2)^{1/6}u \approx 1.55u$ containing about 51% of the total number $\mathcal{N}$ of particles. An estimate of u for $^{87}\mathrm{Rb}$ in a trap of $\Omega = 120 \times 2\pi \, \mathrm{s}^{-1}$ at $T = 5T_{\mathrm{c}} \approx 735 \, \mathrm{nK}$ gives $u \approx 11 \, \mu\mathrm{m}$. Assuming the trap to contain $\mathcal{N} = 2 \times 10^4$ atoms, the peak density will be $n_0 \approx 10^{12} \, \mathrm{cm}^{-3}$ which is typical of the values encountered in cold-atom traps.

For the non-uniform ideal gas considered here, one finds for the average two-particle density ([9], Chap. 2.5)

$$\rho_{\mathcal{N}}^{(2)}(\mathbf{r}, \mathbf{r'}) = \frac{\mathcal{N}(\mathcal{N} - 1)}{(u\sqrt{2\pi})^6} \exp\left(-\frac{\mathbf{r}^2 + \mathbf{r'}^2}{2u^2}\right), \tag{15}$$

implying the two-particle distribution function $g_{\mathcal{N}}^{(2)}(\mathbf{r}, \mathbf{r'}) = 1 - 1/\mathcal{N}$, which is a constant depending on particle number $\mathcal{N}$.
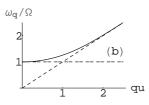
Figure 1. (**a**) Static structure factor; (**b**) characteristic frequency for trapped gas (full line) and free gas (dashed line) and $\omega = \Omega$ (dash–dotted line).

4. Dynamic correlations

It is straightforward to show that the density-fluctuation correlation functions of the non-interacting gas take the simple form

$$F_{\mathbf{q}\mathbf{q}'}(t) = C_{\mathbf{q}\mathbf{q}'}^{(s)}(t) - e^{\frac{1}{2}(q^2 + q'^2)u^2} \tag{16}$$

with $C_{\mathbf{q}\mathbf{q}'}^{(s)}(t) = \frac{1}{N}\sum_{j=1}^{\mathcal{N}}\langle e^{-i\mathbf{q}\cdot\mathbf{r}_j(t)} e^{i\mathbf{q}'\cdot\mathbf{r}_j(0)}\rangle$ denoting the tagged-particle density correlation function, which reduces to

$$C_{\mathbf{q}\mathbf{q}'}^{(s)}(t) = \int d^3\hat{p}\, \frac{\exp(-\frac{\hat{\mathbf{p}}^2}{2p_{\mathrm{T}}^2})}{(p_{\mathrm{T}}\sqrt{2\pi})^3} \int d^3\hat{r}\, \frac{\exp(-\frac{\hat{\mathbf{r}}^2}{2u^2})}{(u\sqrt{2\pi})^3}\{e^{-i\mathbf{q}\cdot\hat{\mathbf{r}}(t)}\, e^{i\mathbf{q}'\cdot\hat{\mathbf{r}}}\}_{\mathrm{av}}, \tag{17}$$

where $\{\cdots\}_{\mathrm{av}}$ explicitly indicates averaging over the stochastic-force variable. Inserting into eq. (17) the solution $\hat{\mathbf{r}}(t)$ according to eq. (A3) with initial time $t_0 = 0$, we obtain

$$C_s(q,t) = C_{\mathbf{q}\mathbf{q}}^{(s)}(t) = \exp\{-q^2u^2[1 - \phi(t)]\} \tag{18}$$

with initial value $C_s(q,0) = 1$ implied by eq. (A7). For non-zero friction, the long-time limiting value $C_s(q,\infty) = \exp(-q^2u^2)$ follows from eq. (A8).

As a consequence, the intermediate scattering function becomes

$$F(q,t) = F_{\mathbf{q}\mathbf{q}}(t) = [e^{q^2u^2\phi(t)} - 1]e^{-q^2u^2}, \tag{19}$$

which is displayed in figure 2 for various Γ and one representative wave number q, will have a damped oscillatory form, in general, with amplitudes ranging between

$$-S(q)\, e^{-q^2u^2} \le F(q,t) \le S(q). \tag{20}$$

It is readily seen from eqs (18), (A8) that $\lim_{t\to\infty} F(q,t) = 0$ for any finite friction constant, and oscillations will be over-damped, if Γ exceeds the aperiodic limit value $\Gamma = 2\Omega$. Evidently, the intermediate scattering function of the trapped ideal gas is closely reflecting the motion of a single gas particle under the influence of friction and harmonic trap potential.

We note that the static structure factor $S(q)$ is not affected by the damping mechanism introduced above. Further, the short-time behaviour,
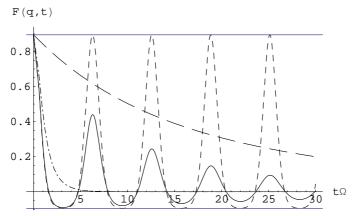
Figure 2. Intermediate scattering functions at wave number $qu = 1.5$ for $\Gamma/\Omega = 0$ (dashed line), 0.1 (full line), 2.01 (dash–dotted line), and 40.0 (long–dashed line). Horizontal lines indicate function range, eq. (20), for this wave number.

$$F(q,t) = S(q)\left[1 - \frac{1}{2}\,\omega_q^2 t^2 + \mathcal{O}(t^3)\right], \quad \omega_q = \frac{qv_{\mathrm{T}}}{\sqrt{S(q)}}\,, \tag{21}$$

is governed by ω_q, the characteristic frequency defined by the second frequency moment $\omega_q^2 := \int\!\mathrm{d}\omega\,\omega^2\phi''(q,\omega)$ of the normalized dynamic structure factor,

$$\phi''(q,\omega) = \pi\frac{S(q,\omega)}{S(q)}\,. \tag{22}$$

The static structure factor, which is vanishing as q^2 for $q \to 0$, is responsible for the gap of size Ω in the graph of ω_q (see figure 1b). Physically, this frequency gap has the following meaning. Long-wavelength excitations of the trapped ideal gas do not constitute propagating density fluctuations (phonons). Instead, a long-wavelength perturbation of the harmonically trapped gas will induce a collective oscillation with frequency Ω of the total gas mass [11]. The appearance of an excitation with frequency ω_q could be thought of as a hybridization of thermal free-particle excitations and the collective oscillation with frequency Ω associated with the trap. With increasing parameter qu, however, this mode will disappear merging into the continuous spectrum,

$$\phi''(q,\omega) \xrightarrow{qu\gg1} \frac{\pi}{S(q)}\,\frac{\exp\left(-\frac{\omega^2}{2\omega_q^2}\right)}{\omega_q\sqrt{2\pi}}, \tag{23}$$

which coincides with the well-known relaxation spectrum of density fluctuations of a uniform ideal gas for $S(q) \equiv 1$ [12]. As qu is increased above one, the characteristic frequency will change its physical significance, because a rapidly growing number of additional resonances at $\omega = 0, \pm2\Omega, \pm3\Omega, \ldots$ will contribute to the second-frequency moment (see eq. (28) below). Eventually, for wave numbers $qu \gg 1$, the
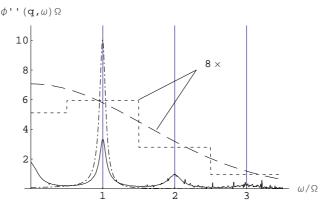
$\phi''(\mathsf{q},\omega)\,\Omega$

Figure 3. Normalized dynamic structure factors at $T = 5T_0$. For $\Gamma/\Omega = 0.1$, at $qu = 1.5$ (full line) from eqs (5) and (22) and $qu = 0$ (dash–dotted line) from eq. (24). Enlarged by factor 8, for $\Gamma/\Omega = 0$, and at $qu = 1.5$: δ-resonances (vertical grid lines) and weights (dashed stairway) from eqs (28), (22), and large-(qu) asymptote (long-dashed line) from eq. (23).
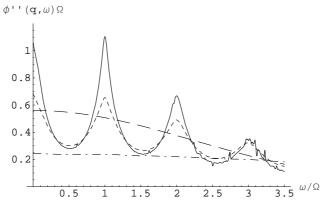
$\phi''(\mathsf{q},\omega)\,\Omega$

Figure 4. Normalized dynamic structure factors for $\Gamma=0.1\,\Omega$, $q=1.5\,u_0^{-1}$ and $T/T_0 = 20, 7$ and 5 (dash–dotted line, dashed line and full line, resp.) from eqs (5) and (22), and for $T/T_0 = 5$ (long-dashed line) from eq. (23).

characteristic frequency $\omega_q \to qv_\mathrm{T}$ will determine the thermal width of the broad Gaussian spectral line centred at zero frequency. Note that the normalized dynamic structure factor has become independent of the trap frequency Ω in the free-particle limit described by eq. (23).

Both $S(q,\omega)$ and $\phi''(q,\omega)$, eq. (22), may be computed from eqs (5), (7) and (18) for arbitrary $q > 0$ and $\Gamma > 0$. An example is given in figure 3 showing $\phi''(q,\omega)$ (full line) at wave number $qu = 1.5$ of a trapped low-friction gas ($\Gamma = 0.1\,\Omega$). It corresponds to the intermediate scattering function which is displayed in figure 2 by a full line, too. Besides the friction-broadened oscillation peak at $\omega = \Omega$, the spectrum clearly exhibits the above-mentioned additional peaks appearing at $\omega = 0$ and 2Ω. These additional peaks are absent in the corresponding spectrum taken

at $qu = 0$, which is also displayed in figure 3. In the long-wavelength limit, the normalized dynamic structure factor may be calculated analytically, since

$$\lim_{q \to 0} \phi''(q,\omega) \equiv \phi''(\omega) := \frac{1}{2} \int_{-\infty}^{\infty} \mathrm{d}t \ \mathrm{e}^{\mathrm{i}t\omega} \ \phi(t) = \frac{\Gamma\Omega^2}{(\omega^2 - \Omega^2)^2 + \omega^2\Gamma^2}, \quad (24)$$

where $\phi''(\omega)$ denotes the relaxation spectrum of the oscillator elongation, which reduces to a pair of δ-functions for vanishing friction constant:

$$\lim_{\Gamma \to 0} \phi''(0,\omega) = \frac{\pi}{2} \left[\delta(\omega - \Omega) + \delta(\omega + \Omega) \right]. \quad (25)$$

For sufficiently small friction, $\phi''(0,\omega)$ describes the collective density excitation at frequency $\omega_{q=0} = \Omega$ exhibited in figure 3 (dash–dotted curve). It should be noted, however, that its detection in a scattering experiment will be difficult due to the small overall scattering intensity $S(q) \approx (qu)^2$ associated with small values of the parameter qu. On the other hand, one has a large overall scattering intensity of $S(q) \approx 0.9$ for $qu = 1.5$, which corresponds to the full curve in figure 3 and to all curves in figure 4.

At non-zero q and sufficiently small Γ, one may speculate the spectrum $\phi''(q,\omega)$ of the form eq. (24) but with $\Omega \to \Omega_q$ and $\Gamma \to \Gamma_q$, where $\Omega_q \approx \omega_q$ as $q \to 0$.

Obviously, the damping mechanism introduced above cannot create positive dispersion ($\Omega_q > \Omega$). Weak frictional and stochastic forces merely achieve broadening of the resonances at $\pm\Omega$ without shifting them. This broadening will only in the over-damped regime lead to an apparent negative dispersion associated with the collapse of peaks at $\omega = 0$ (see eq. (24)).

Figure 4 displays variations of the normalized $S(q,\omega)$ induced by changing the temperature. If $u_0 = \sqrt{k_\mathrm{B}T_0/(m\Omega^2)}$ serves as a unit of length, where T_0 denotes a reference temperature, all T-dependence of the above formulas will be contained in $qu = qu_0\sqrt{T/T_0}$. Choosing a fixed wave number $q = 1.5 \, u_0^{-1}$ and the BEC critical temperature of $\mathcal{N} = 2 \times 10^4$ ^{87}Rb atoms in a trap with $\Omega = 2\pi \times 120\,\mathrm{Hz}$ as a reference, i.e. $T_0 = T_\mathrm{c} \approx 147\,\mathrm{nK}$, the full curve in figure 4 will correspond to $T = 5T_\mathrm{c} \approx 735\,\mathrm{nK}$, a temperature well above the condensation point, where the linear extension of the cloud is $L \approx 28\,\mu\mathrm{m}$.

We note that, for a gas at an ultralow temperature well above T_c, the difference between density-fluctuation spectra of a trapped and a free ideal gas is not only qualitative but also quantitative as the comparison of full and long-dashed curves in figure 4 may demonstrate. This makes us believe that the predicted spectra could be observed in experiments.

Although we chose a small damping constant $\Gamma = 0.1\Omega$ in producing figures 3 and 4, the friction may be unrealistically large, if the results are interpreted as describing an ultracold gas cloud. Instead of producing similar plots from eqs (5) and (22) for much smaller friction constant, which would introduce an increasing amount of difficulties in handling the numerical integration, we will present the analytical solution of the frictionless case in the following section.
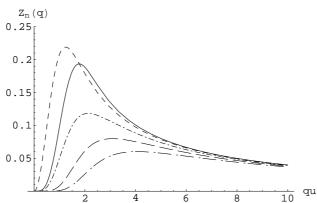
Figure 5. Spectral weights of $S(q, \omega)$ for $n = 0$ (full line), 1 (dashed line), 2 (dash–dotted line), 3 (long-dashed line), 4 (long-dash–dotted line).

5. Undamped motion and DWF

For a purely harmonic trap, one has $\phi(t) = \cos(\Omega t)$ according to eq. (A4). Using this in eq. (19), one obtains the intermediate scattering function

$$F(q, t) = e^{-q^2 u^2} \{\exp[q^2 u^2 \cos(\Omega t)] - 1\} \tag{26}$$

$$= e^{-q^2 u^2} \{I_0(q^2 u^2) - 1 + 2 \sum_{n=1}^{\infty} I_n(q^2 u^2) \cos(n\Omega t)\}, \tag{27}$$

where the generating function of modified Bessel functions of the first kind ([13], Chap. 9.6.34) was applied in the last line. Noting $I_{-n}(z) = I_n(z)$, the dynamic structure factor resulting from eq. (27) reads explicitly:

$$S(q, \omega) = Z_0(q) \, \delta(\omega) + \sum_{n=1}^{\infty} Z_n(q) \, [\delta(\omega - n\Omega) + \delta(\omega + n\Omega)] \tag{28}$$

with spectral weights

$$Z_n(q) := e^{-q^2 u^2} [I_n(q^2 u^2) - \delta_{n,0}] = Z_{-n}(q) \tag{29}$$

corresponding to excitation peaks situated at $\omega = n\Omega$ ($n = 0, \pm 1, \pm 2, \ldots$), which sum up to $\sum_{n=-\infty}^{\infty} Z_n(q) = S(q)$.

Weights are displayed in figure 5 as function of the dimensionless parameter qu. The weights of the elastic and the first inelastic peak at $\omega = \pm \Omega$ have pronounced maxima, while all other $Z_n(q)$ also show a maximum of smaller magnitude around $qu = 2$, decrease to zero slowly for $q \to \infty$, and vanish at $q = 0$. For $|n| \geq 1$, they decrease with increasing n. Further, it can be seen that Z_1 clearly dominates the inelastic-scattering weights Z_n in the range of small wave numbers, $1 > qu > 0$. In the long-wavelength limit, finally, the collection of infinitely many resonances will collapse into a pair at $\omega = \pm \Omega$, in accordance with eq. (25). That is easily verified by applying the limiting values
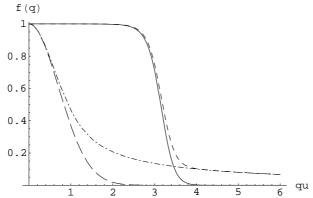
Figure 6. Debye–Waller factor of $\mathcal{N} = 2 \times 10^4$ atoms in harmonic trap for $\Gamma > 0$ (full line) and $\Gamma = 0$ (dashed line). DWF of single trapped atom ($\mathcal{N} = 1$) for $\Gamma > 0$ (long-dashed line) and $\Gamma = 0$ (dash–dotted line).

$$\lim_{q \to 0} \frac{Z_n(q)}{S(q)} = \frac{1}{2}\,\delta_{|n|,1}, \tag{30}$$

in eq. (28) from which one finds

$$S(q, \omega) \longrightarrow (q^2 u^2/2)\,[\delta(\omega - \Omega) + \delta(\omega + \Omega)] \tag{31}$$

for $qu \ll 1$. Spectral weights $\pi Z_n(q)/S(q)$ corresponding to $\phi''(q, \omega)$ have been indicated for $qu = 1.5$ in figure 3 in terms of a 'stairway' spectral function together with the continuous spectrum eq. (23). Plotting a sequence of such stairways for increasing values of the parameter qu will provide a good visualization of the spectrum metamorphosis from a sum of only a few visible stairs for $qu < 1$ to the continuous broad spectrum of the uniform ideal gas for $qu \gg 1$.

It is to be noted that for the purely harmonic trap the dynamical structure factor $S(q, \omega)$ defined by the temporal Fourier transform of the correlation function of density fluctuations, eq. (5), will contain an elastic scattering contribution due to $F(q, \infty) \neq 0$, which is absent for $\Gamma > 0$. This contribution, together with the *a priori* elastic contribution $\delta(\omega)|\langle N_{\mathbf{q}} \rangle|^2/\mathcal{N}$ to the coherent double-differential scattering cross-section, when used in eq. (6), will lead to DWF of the trapped ideal gas

$$f(q) = \frac{e^{-q^2 u^2}\left[I_0(q^2 u^2) + \mathcal{N} - 1\right]}{1 + (\mathcal{N} - 1)e^{-q^2 u^2}}, \tag{32}$$

whereas for $\Gamma > 0$ the bracket in the numerator of eq. (32) is simply replaced with $\mathcal{N}$. Contrary to a homogeneous gas, the DWF of the trapped atomic cloud does not vanish and depends on $\mathcal{N}$. The DWF is displayed for a trapped cloud of $\mathcal{N} = 20{,}000$ atoms in figure 6. For comparison, also the DWF of a single trapped atom ($\mathcal{N} = 1$) is given, which coincides with the Lamb–Mößbauer factor (LMF) of the trapped ideal gas.

6. Concluding remarks

In this paper we have calculated the density-fluctuation spectrum of a classical ideal gas in a harmonic potential at temperatures well above the BEC temperature, but in a micro-Kelvin range which is still of interest. In this regime, $\hbar\Omega$ is much less than $k_{\mathrm{B}}T$ for trapped atomic gases. It is found that the difference between the density fluctuation spectra of the trapped and the free gas is large enough to be observed experimentally. The calculation predicts the existence of density excitations of the trapped mass which increases with increasing wave number. It is shown that Debye–Waller factor for trapped thermal clouds of $\mathcal{N}$ atoms are finite contrary to a homogeneous gas, opening the possibility of observing recoilless emission of ultralow frequency radiation from the trapped gas. It is hoped that this work will stimulate interest in performing inelastic scattering experiments.

Appendix A: Time evolution of $\vec{\mathbf{r}}(t)$ and $\vec{\mathbf{p}}(t)$

In order to evaluate eq. (17), we need to know the time evolution of particle position $\hat{\mathbf{r}}(t) = \mathbf{R}(\hat{\mathbf{p}}, \hat{\mathbf{r}}, t)$ and momentum $\hat{\mathbf{p}}(t) = \mathbf{P}(\hat{\mathbf{p}}, \hat{\mathbf{r}}, t)$. In the present case of an isotropic oscillator potential, the vector components of $\hat{\mathbf{r}}(t)$ as well as of $\hat{\mathbf{p}}(t)$ are not coupled. Therefore, we outline the method of evaluation of the x-components $\hat{x}(t)$ and $\hat{p}_x(t)$, only. The same method applies to the y- and z-components.

In the presence of a driving force $\mathcal{F}_x(t)$, the elongation $\hat{x}(t)$ will obey the damped driven oscillator equations of motion,

$$\frac{\mathrm{d}}{\mathrm{d}t}\hat{x}(t) = \frac{1}{m}\hat{p}_x(t) \tag{A1}$$

$$\frac{\mathrm{d}}{\mathrm{d}t}\hat{p}_x(t) = -m\Omega^2\hat{x}(t) - m\Gamma\,\frac{\mathrm{d}}{\mathrm{d}t}\hat{x}(t) + \mathcal{F}_x(t), \tag{A2}$$

with the unique solution

$$\hat{x}(t) = \phi(t - t_0)\,\hat{x} + \mathrm{i}\chi(t - t_0)\,\hat{p}_x + \int_{t_0}^{t}\mathrm{d}t'\,\mathrm{i}\chi(t - t')\,\mathcal{F}_x(t') \tag{A3}$$

corresponding to initial conditions $\hat{x}(t_0) = \hat{x}$ and $\hat{p}_x(t_0) = \hat{p}_x$. Here $\phi(t)$ and $\chi(t)$, defined by ($t \geq 0$)

$$\phi(t) := \frac{z_1 \mathrm{e}^{z_2 t} - z_2 \mathrm{e}^{z_1 t}}{z_1 - z_2}\,, \qquad \chi(t) := \frac{1}{\mathrm{i}m}\,\frac{\mathrm{e}^{z_1 t} - \mathrm{e}^{z_2 t}}{z_1 - z_2}\,, \tag{A4}$$

$$z_{1,2} = -\Gamma/2 \pm \sqrt{(\Gamma/2)^2 - \Omega^2}\,, \tag{A5}$$

denote the (normalized) relaxation function and the linear response function of the oscillator elongation, respectively. Equations similar to eq. (A3) also apply for the y- and z-components.

Indeed, $\phi(t)$ represents the normalized Kubo relaxation function of elongation. This can be seen as follows. Choosing $t_0 = 0$ in eq. (A3), multiplying with $\hat{x}/(k_{\mathrm{B}}T)$ on both sides and subsequently taking a thermal average will – on the left-hand

side – result in the Kubo relaxation function of elongation, $\Phi(t) = \langle \hat{x}(t)\hat{x} \rangle / (k_B T)$. On the right-hand side, only the first term $\phi(t)\langle \hat{x}^2 \rangle / (k_B T) \equiv \phi(t)\Phi(0)$ will survive, where $\Phi(0) = 1/(m\Omega^2)$.

Both functions, $\phi(t)$ and $\chi(t)$, are related by Kubo's identity,

$$\chi(t) = \frac{i\dot{\phi}(t)}{m\Omega^2},$$ (A6)

which can be verified explicitly for the results given in eq. (A4). Also, the initial values of the relaxation function,

$$\phi(0) = 1, \quad \dot{\phi}(0) = 0,$$ (A7)

can be read from eqs (A4) and (A6), while one has

$$\phi(\infty) = 0, \quad \dot{\phi}(\infty) = 0, \quad (\Gamma > 0)$$ (A8)

for finite friction. The magnitude of the normalized relaxation function is restricted to the interval $[0,1]$ or, equivalently,

$$-1 \le \phi(t) \le 1$$ (A9)

for any time t.

In addition to the restoring force and the friction force, it has been assumed in eq. (A2) that there acts a time-dependent random force $\mathcal{F}_x(t)$ on the oscillator. Thermal averaging is then understood to include additional averaging over stochastic variables as indicated explicitly in eq. (17). For evaluating the stochastic average, we assumed that the driving force $\mathcal{F}_x(t)$ represents Gaussian white noise, which after straightforward calculation leads to the result eq. (18).

Appendix B: Non-diagonal correlation functions

Assuming undamped oscillations

$$\hat{\mathbf{r}}(t) = \cos(\Omega t)\,\hat{\mathbf{r}} + \frac{\sin(\Omega t)}{m\Omega}\,\hat{\mathbf{p}},$$ (B1)

one finds from eqs (16) and (17)

$$F_{\mathbf{q}\,\mathbf{q}'}(t) = e^{-\frac{1}{2}(q^2+q'^2)u^2}[e^{\mathbf{q}\cdot\mathbf{q}'u^2\cos(\Omega t)} - 1],$$ (B2)

which by Fourier transformation leads to

$$F(\mathbf{r},\mathbf{r}',t) = \left[\frac{\exp\left(-\frac{[\mathbf{r}-\mathbf{r}'\cos(\Omega t)]^2}{2u^2\sin^2(\Omega t)}\right)}{\left(u|\sin(\Omega t)|\sqrt{2\pi}\right)^3} - \frac{\exp\left(-\frac{\mathbf{r}^2}{2u^2}\right)}{\left(u\sqrt{2\pi}\right)^3} \right] \frac{\exp\left(-\frac{\mathbf{r}'^2}{2u^2}\right)}{\left(u\sqrt{2\pi}\right)^3}.$$ (B3)

It is noted that $F_{\mathbf{qq'}}(t) = F_{\mathbf{q'q}}(t)$ and $\lim_{q\to 0} F_{\mathbf{qq'}}(t) = 0$. We further observe $\int\mathrm{d}^3 r\, F(\mathbf{r}, \mathbf{r}', t) = \int\mathrm{d}^3 r'\, F(\mathbf{r}, \mathbf{r}', t) = 0$.

Taking the limit $t \to 0$ in eq. (B3) one finds

$$F(\mathbf{r}, \mathbf{r}', 0) = \left[\delta(\mathbf{r} - \mathbf{r}') - \frac{\exp\left(-\frac{\mathbf{r}^2}{2u^2}\right)}{\left(u\sqrt{2\pi}\right)^3}\right] \frac{\exp\left(-\frac{\mathbf{r}'^2}{2u^2}\right)}{\left(u\sqrt{2\pi}\right)^3} \tag{B4}$$

which is the inverse Fourier transform of eq. (12) or of the $t = 0$-value of eq. (B2).

Acknowledgements

References

[1] C J Pethick and H Smith, *Bose–Einstein condensation in dilute gases* (Cambridge University Press, Cambridge, 2002)
[2] Lev Pitaevskii and Sandro Stringari, *Bose–Einstein condensation* (Clarendon Press, Oxford, 2003)
[3] M Greiner, C A Regal and J T Stewart, *Phys. Rev. Lett.* **94**, 110401 (2005)
[4] P B Blakie, R J Ballagh and C W Gardiner, *Phys. Rev.* **A65**, 33602 (2002)
[5] C Menotti, M Krämer, L Pitaevskii and S Stringari, *Phys. Rev.* **A67**, 53609 (2003)
[6] Jean-Sébastien Caux and Pasquale Calabrese, *Phys. Rev.* **A74**, 31605 (2006)
[7] Gyula Bene and Péter Széfalusy, *Phys. Rev.* **A58**, R3391 (1998)
[8] D Pines and P Nozières, *The theory of quantum liquids* (W A Benjamin, Inc., New York, 1966)
[9] J P Hansen and I R McDonald, *Theory of simple liquids* (Academic Press, London and New York, 2005) 3rd edition
[10] P A Egelstaff, *An introduction to the liquid state* (Oxford Science Publications, Clarendon Press, Oxford, 1994) 2nd edition
[11] This is analogous to charge-density excitations in a one-component plasma where, in the long-wavelength limit, the charge density will perform oscillations with the plasma frequency due to restoring Coulomb forces created by the charge-neutralizing background (see, e.g. [14])
[12] A derivation of eq. (23) in the present context is straightforward. Starting from $F(q,t)|_{\Gamma=0}$ given in eq. (26), inserting $u = v_{\mathrm{T}}/\Omega$ and $\cos(\Omega t) \to 1 - \Omega^2 t^2/2$ for small Ω, and performing the free-particle limit $\Omega \to 0$, immediately results in $F(q,t) = \exp(-q^2 v_{\mathrm{T}}^2 t^2/2)$ for a free ideal gas which implies eq. (23)
[13] Milton Abramowitz and Irene A Stegun (Eds), *Handbook of mathematical functions* (Dover Publications, Inc., New York, 1970)
[14] J Bosse and K Kubo, *Phys. Rev. Lett.* **40**, 1660 (1978)